Insight into the structural, electronic, elastic and optical properties of the alkali hydride compounds, XH (X = Rb and Cs)

Raed Jaradat, Mohammed Abu-Jafar, Issam Abdelraziq, Ahmad Mousa, Tarik Ouahrani, and Rabah Khenata

Citation: AIP Advances **8**, 045017 (2018); doi: 10.1063/1.5025002
View online: https://doi.org/10.1063/1.5025002
View Table of Contents: http://aip.scitation.org/toc/adv/8/4
Published by the American Institute of Physics

Insight into the structural, electronic, elastic and optical properties of the alkali hydride compounds, XH (X = Rb and Cs)

Raed Jaradat,[1] Mohammed Abu-Jafar,[1,a] Issam Abdelraziq,[1] Ahmad Mousa,[2] Tarik Ouahrani,[3] and Rabah Khenata[4]
[1]*Physics Department, An-Najah National University, P. O. Box 7, Nablus, Palestine*
[2]*Middle East University, Amman 11831, Jordan*
[3]*Ecole Supérieure en Sciences Appliquées, B. P. 165, 13000 Tlemcen, Algeria*
[4]*Laboratoire de Physique Quantique de la Matière et de la Modélisation Mathématique (LPQ3M), Université de Mascara, Mascara 29000, Algeria*

(Received 6 February 2018; accepted 9 April 2018; published online 19 April 2018)

The equilibrium structural parameters, electronic and optical properties of the alkali hydrides RbH and CsH compounds in rock-salt (RS) and cesium chloride (CsCl) structures have been studied using the full-potential linearized augmented plane-wave (FP-LAPW) method. Wu and Cohen generalized gradient approximation (WC-GGA) was used for the exchange-correlation potential to compute the equilibrium structural parameters, such as the lattice constant (a_0), the bulk modulus (B) and bulk modulus first order pressure derivative (B'). In addition to the WC-GGA, the modified Becke Johnson (mBJ) scheme has been also used to overcome the underestimation of the band gap energies. RbH and CsH compounds are found to be semiconductors (wide energy-band gap) using the WC-GGA method, while they are insulators using the mBJ-GGA method. Elastic constants, mechanical and thermodynamic properties were obtained by using the IRelast package. RbH and CsH compounds at ambient pressure are mechanically stable in RS and CsCl structures; they satisfy the Born mechanical stability criteria. Elastic constants (C_{ij}), bulk modulus (B), shear modulus (S) and Debye temperatures (θ_D) of RbH and CsH compounds decrease as the alkali radius increases. The RS structure of these compounds at ambient conditions is mechanically stronger than CsCl structure. RbH and CsH in RS and CsCl structures are suitable as dielectric compounds. The wide direct energy band gap for these compounds make them promising compounds for optoelectronic UV device applications. Both RbH and CsH have a wide absorption region, on the other hand RbH absorption is very huge compared to the CsH absorption, RbH is an excellent absorbent material, maximum absorption regions are located in the middle ultraviolet (MUV) region and far ultraviolet (FUV) region. The absorption coefficient α (w), imaginary part of the dielectric constant $\varepsilon_2(w)$ and the extinction coefficient k(w) vary in the same way. The present calculated results are in good agreement with the experimental data, indicating the high accuracy of the performed calculations and reliability of the obtained results. https://doi.org/10.1063/1.5025002

I. INTRODUCTION

The alkali hydrides compounds XH (X=Li, Na, K, Rb, and Cs) are very interesting compounds. They have the simplest electronic structure. These compounds, alkaline earth metal hydrides as BeH_2, transition metal hydrides as TiH_2 and metal tri-hydrides as AlH_3 have attracted researchers in different

[a]Corresponding author: mabujafar@najah.edu (Mohammed S. Abu-Jafar)

areas due to their wide range of applications. They can be used as electrodes of rechargeable batteries, shielding materials of radiation. Alkali hydrides along with complex hydrides are also interesting for their capacity to store hydrogen.[1–6] The diamond-anvil-cell study showed that XH compounds crystallize in RS structure at room temperature.[7–9] For better understanding of the optical properties, the electronic properties have been calculated. Gulebaglan *et al.*[10] carried out first-principles calculations to obtain the optical properties of RbH compound in RS structure. Their calculated static refractive index n(0) value is 1.75 for low energy electromagnetic waves. The absorption coefficient α(w) and the extinction coefficient k(w) vary in the same way, there is no electromagnetic waves absorption through 2.93eV. Van Setten *et al.*[11] studied the dielectric functions of the LiH and NaH in RS structure by using first-principles density functional theory and all-electron GW approximation. A differences between the band structures of NaH and LiH have been found, which lead to a clearly different dielectric functions. The energy band structure of LiH is more dispersed than that of NaH, as a result, imaginary part of the dielectric functions of the LiH is spread out over a larger energy range. Xinyou *et al.*[12] used the generalized gradient approximation (GGA) to calculate the optical properties of KH compound in both RS and CsCl structures. Both RS and CsCl structures have a wide absorption region starting at about 3.28 eV and 2.51eV for RS and CsCl, respectively.

Their calculated static refractive index n(0) for KH in RS and CsCl structures are around 1.50 and 1.70, respectively. They found it unsuitable as transparent material and optical properties vary with pressure. From the above, it is clear that the optical properties for the family of alkali hydride compounds have been done for only the NaH and LiH compounds in the RS structure and the KH in both RS and CsCl phase.

To the best of our knowledge, there are no experimental and theoretical calculations for the optical properties of the RbH and CsH compounds reported in the literature in RS and CsCl structures. Moreover, experimental information regarding the structural properties as well as the elastic constant and their related properties of RbH and CsH compounds in the CsCl structure are not available. The reasons mentioned above motivates us to perform the calculations on the structural, electronic and the optical properties of RbH and CsH in RS and CsCl structures, in order to provide additional data for the existing theoretical works on these compounds, using the full-potential augmented plane wave method (FP-LAPW).

This paper is organized as follows: in Section II, we give a brief description of the used computational technique. The Section III is reserved to the presentation and discussion of the obtained results on the structural, electronic, elastic and optical properties of RbH and CsH compounds. Finally, in Section IV, we summarize the main conclusions drawn from this study.

II. METHOD OF CALCULATION

Developments in theoretical computational methods now a day's in the electronic structure overcome calculations problems. As a result this has led to a new class of first-principles approaches; this enables us to calculate the optical properties. The calculations reported here were carried out using the full potential linearized augmented plane wave (FP-LAPW), implemented in WIEN2K package.[13] In this method the atomic space of the system is divided into an interstitial region (IR); often called Muffin-tin sphere, space occupied by atomic spheres with radius R_{MT}; and region outside the spheres, non-overlapping muffin tin (MT) spheres.

In the interstitial region, the basis set consists of plane waves, while in the non-overlapping region, the basis sets can be described by a linear combination of radial functions of the one particle Schrödinger equation along with their energy derivatives multiplied by spherical-harmonics. The exchange correlation potential (V_{XC}) effects for the ground state properties are treated by two approximations, the Wu–Cohen generalized gradient approximation (WC-GGA) and the modified Becke–Johnson (mBJ-GGA) formalism.[14,15] In the IR and MT regions, in order to get sufficient and appropriate energy convergence, the basis set functions of the system were expanded up to $R_{MT}\times K_{Max}=5$, where K_{Max} gives the magnitude of the maximum k-vector value used in the plane wave and R_{MT} is the radius of the MT spheres in the unit cell. Inside the atomic sphere, the charge density was Fourier expanded up to $G_{max}= 22$ with a cut-off $l_{max} = 6$. Calculating the total energy

of the unit cell was iterated and repeated until the self-consistent calculations converged to less than 10^{-5} Ry/unit cell. The energy which separates core and valence states from each other is 6.0 Ry. For energy convergence, the number of k-points for the cubic structure in the full Brillouin zone (FBZ) was taken 2000, which is reduced to 56 special k-points in the irreducible Brillouin zones (IBZ).[16] The valence electron configurations of RbH are: Rb $4s^2$, $4p^6$, $5s^1$ and H $1s^1$, while for CsH the valence electron configurations are: Cs $4d^{10}$, $5s^2$, $5p^6$, $6s^1$ and H $1s^1$.

III. RESULTS AND DISCUSSIONS

A. Structural properties

The ground state properties of the alkali compounds XH have been calculated by using the FP-LAPW method at the level of Wu-Cohen-GGA (WC-GGA) approximation, which is a GGA improved and was proposed by Walter Kohen.[14,17] The calculations were performed for cubic (RS and CsCl) structures. Murnaghan's equation of state (EOS)[13] has been used to estimate the equilibrium lattice constant (a_0) bulk modulus (B) and its first order pressure derivative (B′) as displayed in Tables I and II for RbH and CsH, respectively.

The computed lattice constant, bulk modulus and its first order pressure derivative are in fairly good agreement with experimental results[7,9,18–20] and other theoretical calculations.[10,21–24] The experimental lattice constant for RbH and CsH in RS structure overestimates the present result by about

TABLE I. Structural parameters for RbH in RS and CsCl structures, along with experimental and other theoretical results.

Structure	Structural parameters	Present work	Experimental work	Other theoretical work
RS	a_0(Å)	5.94	6.037[a], 6.048[b]	5.992[c], 6.064[d]
	B_0(GPa)	12.14	10.0 ± 1.0[e]	14.1[c], 14.7[f]
	B'	4.38	3.9 ± 0.5[e]	2.840[c]
CsCl	a_0(Å)	3.52	.....	3.81[c]
	B_0(GPa)	14.67	18.4 ± 1.1[e]	14.9[c]
	B'	3.98	3.9 + 0.5[e]	2.866[c]

[a]Reference 18,
[b]Reference 19,
[c]Reference 24,
[d]Reference 10,
[e]Reference 9,
[f]Reference 21.

TABLE II. Structural parameters for CsH in RS and CsCl structures, along with experimental and other theoretical results.

Structure	Structural parameters	Present work	Experimental work	Other theoretical work
RS	a_0(Å)	6.27	6.387[a,b], 6.376[b]	6.344[c], 6.407[d]
	B_0(GPa)	10	8.0± 0.7[a], 7.6 ±0.8[e]	12[c], 11.9[f], 8.8[g]
	B'	3.70	4.0[a], 4 ± 0.4[e], 4.0[h]	3.037[c]
CsCl	a_0(Å)	3.72	.....	3.84[c]
	B_0(GPa)	14.2	14.2± 1[a], 22.3 ± 1.5[e] 15.9[i]	14[c]
	B'	4.91	4 ± 0.2[a], 4.8 ± 0.5[e]	4.675[c]

[a]Reference 7,
[b]Reference 18,
[c]Reference 24,
[d]Reference 23,
[e]Reference 9,
[f]Reference 21,
[g]Reference 22,
[h]Reference 19,
[i]Reference 20.

0.097 Å (1.6%) and 0.11 Å (1.7%), respectively. This is mainly related to two main reasons: the difference in the temperatures used in the experimental and theoretical calculations and the difference in the pressures used. As it can be seen from Tables I and II, the a_0 value of RbH is smaller than CsH: a_0(RbH) < a_0(CsH). The result can be easily explained by considering the atomic radii of Cs and Rb: R(Rb) =2.65 Å, R(Cs) =2.98 Å. Meanwhile, the bulk modulus B values for RbH is greater than CsH; B(RbH) > B(CsH), i.e. in inverse sequence to a_0 - in agreement with the well-known relationship between B and the lattice constants: $B \propto V_0^{-1}$, where V_0 is the unit cell volume.

B. Formation and cohesive energy

Studying the relative phase stabilities for any compound can be deduced from the formation energy (E_{form}). The formation energy is defined as:

$$E_{form}^{XH} = E_{tot}^{XH} - \sum n_i \mu_i \tag{1}$$

Where, E_{tot}^{XH} is the total energy of the XH per formula in CsCl and RS phases, n_i is the number of atoms for each constituent in the compound (in our case n_i=*1*), and μ_i is the stable bulk phase chemical potential (both Cs and Rb are in bcc structure and H in hcp structure).

The results from this equation are summarized in Table III. From this table one can see that the RS phase is more stable than the CsCl phase for each compound, on the other hand two phases (CsCl and RS phases) have a negative formation energy, which indicates that it is possible to exist in nature.

The cohesive energy is a measure of the strength of the forces that bind atoms together in the solid state and is descriptive in studying the phase stability. The cohesive energy (E_{coh}) is defined as the total energy of the constituent atoms minus the total energy of the compound:

$$E_{coh}^{XH} = \left(aE_{atom}^{X} + bE_{atom}^{H}\right) - E_{tot}^{XH} \tag{2}$$

Where E_{coh}^{XH} is the total energy of the unit cell used in the present calculations, a and b are the numbers of (Cs, Rb) and H atoms in unit cell, respectively. E_{tot}^{XH} refers to the total energy of XH compound in the equilibrium configuration. E_{atom}^{X} and E_{atom}^{H} are the isolated atomic energies of the pure constituents. The calculated cohesive energies are presented in Table III. From these results one can see that the bind atoms together in the RS phase is larger than the bind atoms in the CsCl phase.

On the other hand, in Table III we calculate the weight percentage of hydrogen (Hydrogen Storage Capacity), it is easy to see that the hydrogen weight in one mole of RbH is larger than one mole of CsH. Their high hydrogen content and lower weight make RbH attractive for portable applications.[25]

C. Electronic properties

The electronic properties of RbH and CsH with the RS and CsCl structures have been calculated in order to estimate their optical properties. The knowledge of the electronic properties of a material is essential to understand its optical properties. The equilibrium lattice constant (a_0) for the RS and CsCl phases has been used to calculate the energy band structures for RbH and CsH compounds. It is well known that energy band structure is underestimated with both GGA and LDA approaches and insulating state sometimes may obtained with GGA and LDA as a semiconducting state, or even metallic one.[26] This problem in GGA and LDA increases the Coulomb potential by shifting the Rb

TABLE III. The formation and cohesive energy for XH compound in CsCl and RS phases.

Compound	Phase	(eV/formula) E_{form}	(eV/formula) E_{coh}	Weight percentage of hydrogen %
CsH	CsCl	-1.398	3.387	0.75
	RS	-1.439	3.429	
RbH	CsCl	-1.271	3.305	0.98
	RS	-1.347	3.380	

and Cs energy states to higher levels due to the limitations in the GGA and LDA methods, because of the discontinuity in the energy derivative for certain electrons.[26] An exact exchange potential has been suggested by Becke and Johnson to solve this problem which reduces the Coulomb repulsion between the s states of the atoms in the compound.[14,15] For better energy band structure calculations, Wu-Cohen-GGA and mBJ-GGA approaches for the exchange-correlation potential have been used. The band structures for RbH and CsH with the two structures, RS and CsCl are calculated along the high symmetry directions of the first Brillouin zone as shown in Figures 1 and 2. These compounds have a direct minimum energy-band gap with RS structure along the L-point symmetry line (the optical transitions are direct). The minimum energy band gap for RbH with CsCl is an indirect from the R to X-point symmetry line with both WC-GGA and mBJ-GGA approximations, while the CsH with CsCl structure has a direct minimum energy band gap along the R-point symmetry line using both mBJ-GGA and WC-GGA approximations.

The Fermi energy level is chosen to coincide with the zero energy, by comparison with WC-GGA, the energy band gaps with mBJ-GGA are wider with both structures RS and CsCl; WC-GGA has shifted the valence and conduction bands closer to one another as shown in Figures 1 and 2. The calculated minimum energy band gap values for both RbH and CsH in RS and CsCl structures with the two approaches, mBJ-GGA and WC-GGA are reported in Table IV along with the results of

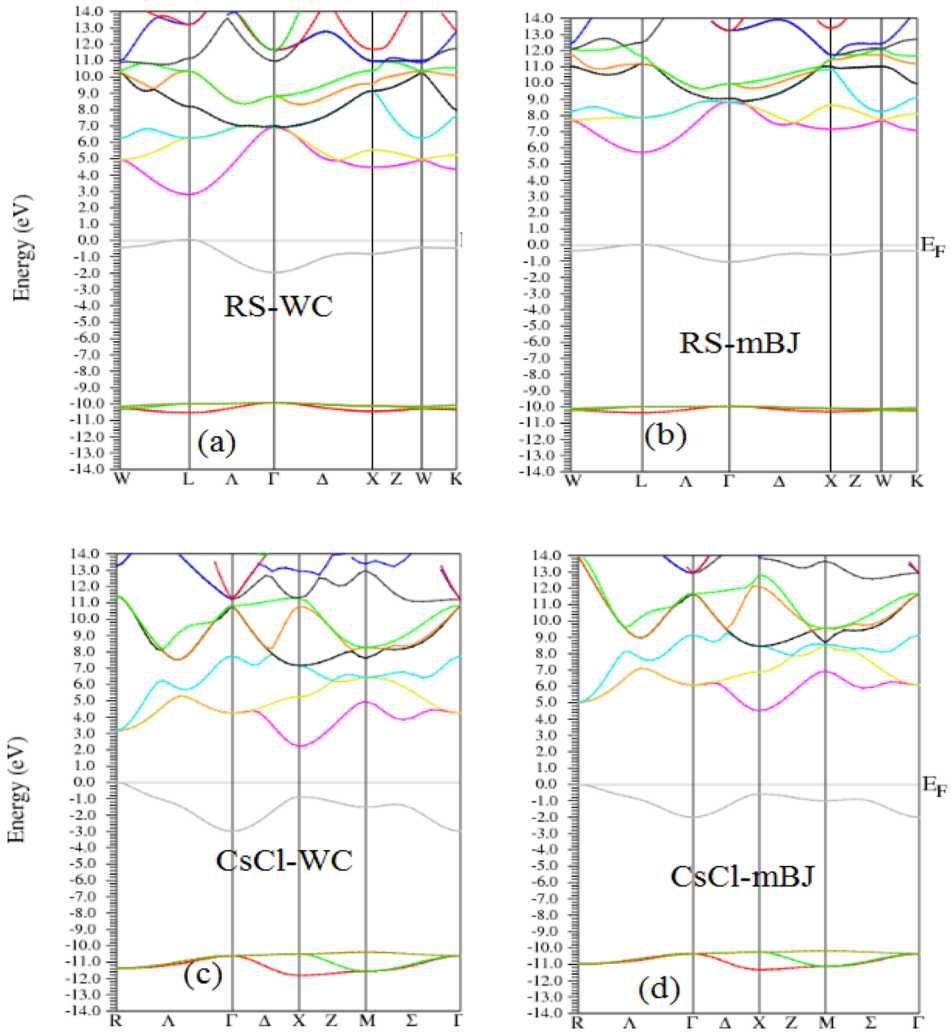

FIG. 1. Band structure of RbH in RS structure using a) WC-GGA b) mBJ-GGA and in CsCl structure using c) WC-GGA d) mBJ-GGA.

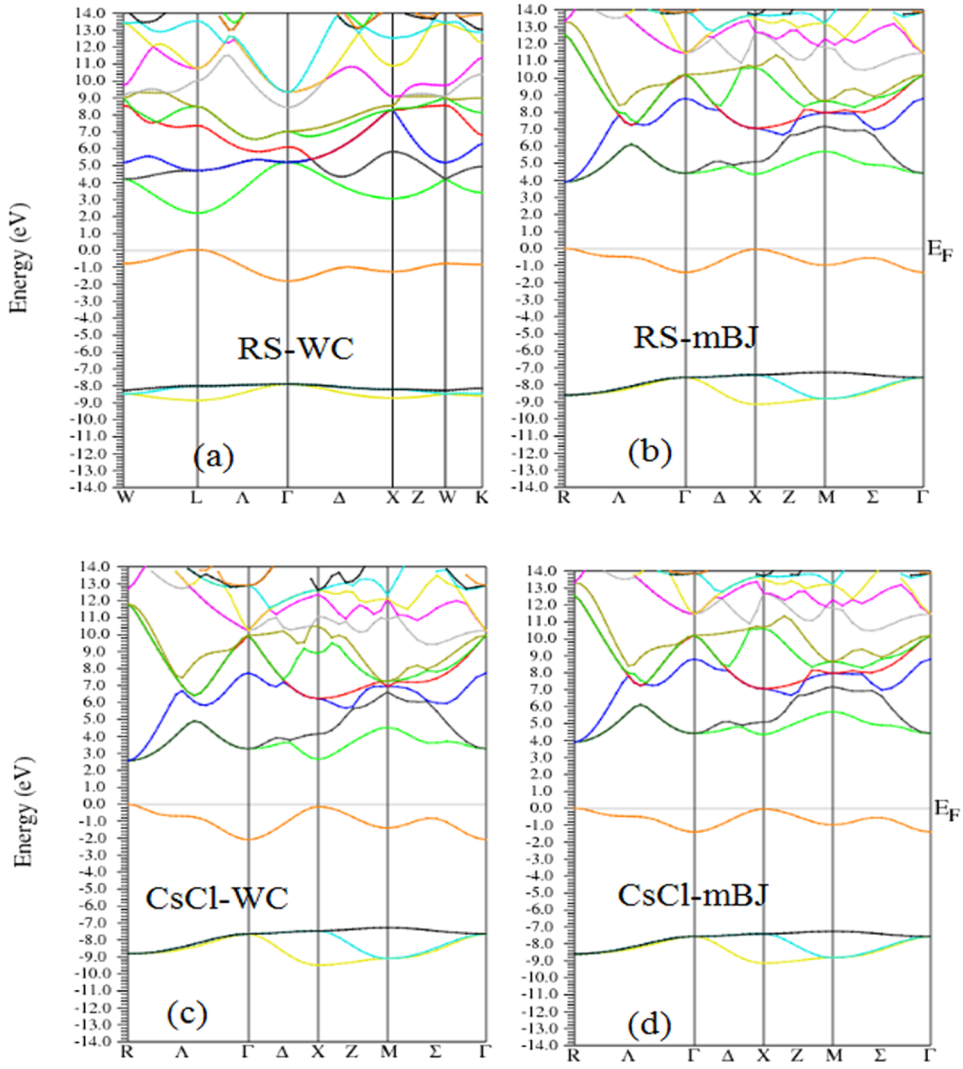

FIG. 2. Band structure of CsH in RS structure using a) WC-GGA b) mBJ-GGA and in CsCl structure using c) WC-GGA d) mBJ-GGA.

previous theoretical[24,27–30] and experimental[31,32] works. The energy-band gaps with mBJ-GGA are broader than results with WC-GGA by about 1.16eV to 2.583eV, depending on which structure has been used. The energy band gap values for RbH with RS and CsCl structures are about 3.050 eV and 2.397 eV (mBJ: 5.663 eV and 4.474 eV), respectively, while for CsH they are 2.26eV and 2.56 eV (mBJ: 4.59eV and 3.72eV), respectively. The calculated energy-band structure has been modified by using the exact exchange-correlation potential; mBJ-GGA approach; as a result, the calculated band gaps with mBJ-GGA approach agree well with the experimental results. The differences in calculating the energy band gap between the experiment and mBJ-GGA approach are about 0.7eV and 0.19eV for RbH and CsH, respectively, this is mainly due to the very small variation between the computed lattice constant and experimental data. Our present mBJ-GGA energy band gap values are more accurate than those obtained in other theoretical work, results in Refs. 24 and 27 are smaller than experimental result by about 2eV, while results in Ref. 29 are greater than experimental result by about 2eV. RbH and CsH are classified as a semiconductors or wide band gap semiconductor using WC-GGA method, while mBJ-GGA method categorized them as insulators. The calculated partial and total density of states (DOSs) for RbH and CsH compounds are shown in Figures 3 and 4, respectively. DOSs for a certain system usually used to describes the number of states that are available to be occupied at each energy level. It is clear that the DOSs can be mainly divided into two

TABLE IV. Calculated energy band-gap values ((Eg(eV)) for RbH and CsH with RS structure along L→L direction and in CsCl structure along R→X direction.

Compound	Structure	Energy band gap (E_g) WC-GGA	mBJ-GGA	Other theoretical work (E_g)	Experimental results (E_g)
RbH	RS	3.050	5.633	3.0255[a], 2.960[b], 4.21[c]	4.91[d]
	CsCl	2.397	4.474	6.97[e]	---------
				2.1[a]	
CsH	RS	2.27	4.59	2.4472[a], 4.04[c], 6.67[e],	4.4[f]
	CsCl	2.56	3.72	2.80[g]	------
				2.5[a]	

[a]Reference 24,
[b]Reference 27,
[c]Reference 28,
[d]Reference 31,
[e]Reference 29,
[f]Reference 32,
[g]Reference 30.

parts, valence band; the bands below the Fermi energy level (FE); and conduction band; the bands above the Fermi energy level (FE). The valence band for XH compound, Figures 3 and 4, made mainly from H-s states along with some contribution from X-s and X-p states, while the conduction band dominate with X-d with a small contribution from X-p and H-s states.

While the majority of the hydrides are rather pure covalent[33] or metallic when they bond with transition metals,[33] our titled compounds as far as they are concerned belong to group I.[33] In this group, the compounds have rather some ionicity in their chemical bonds, known as saline hydrides or pseudohalides. The reason of this behavior is that the hydrogen atoms act as the hydride ions (H^-) which bond with more electropositive alkaline-earth metals, here the rubidium and cesium ones. Thus, in order to give deeper analysis on this bonding, we will make in this subsection an extensive use of state of the art quantum interpretative techniques based topological analysis of the electron density (ρ).

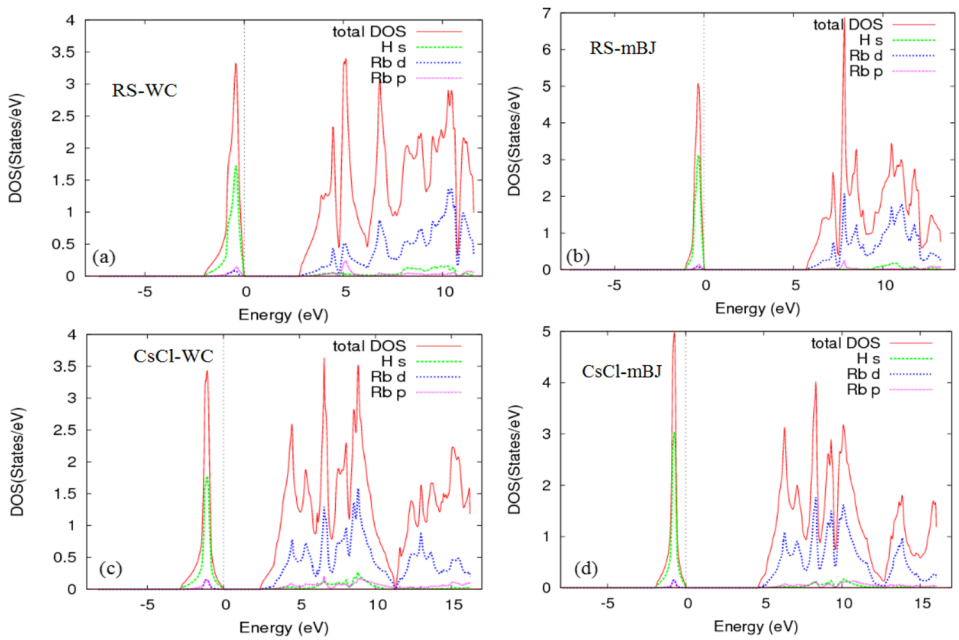

FIG. 3. Density of states (DOS) of RbH in RS structure using a) WC-GGA b) mBJ-GGA and in CsCl structure using c) WC-GGA d) mBJ-GGA.

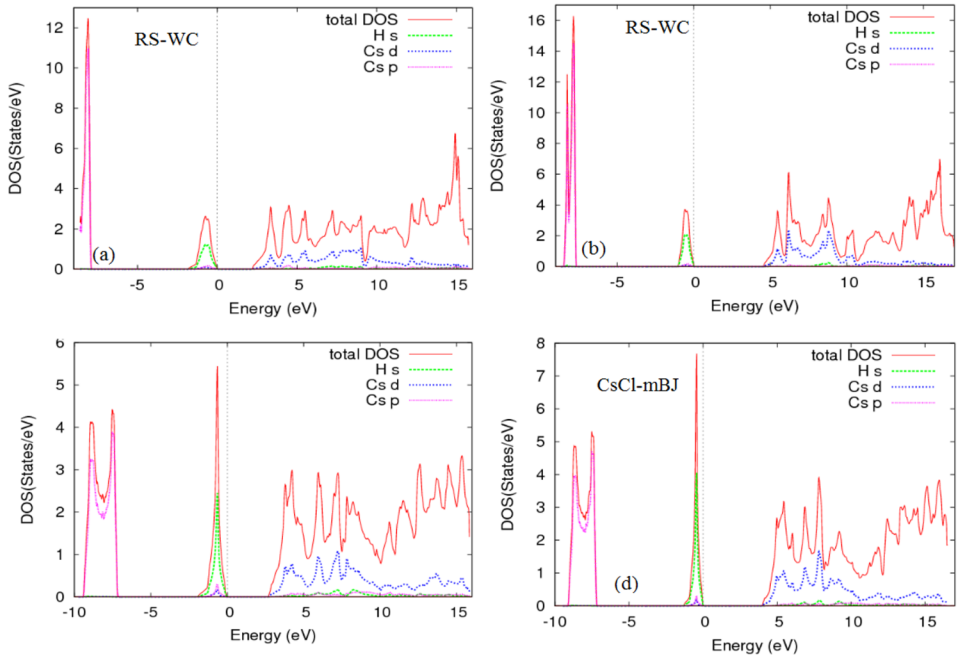

FIG. 4. Density of states (DOS) of CsH in RS structure using a) WC-GGA b) mBJ-GGA and in CsCl structure using c) WC-GGA d) mBJ-GGA.

The most prominent approaches are the quantum theory of atoms in molecules (QTAIM).[34] QTAIM divides direct space into discrete atomic basins, which predicts self-consistent local properties such as charges and volumes, likewise a topological inter-atomic bond path motif, which is attributed to

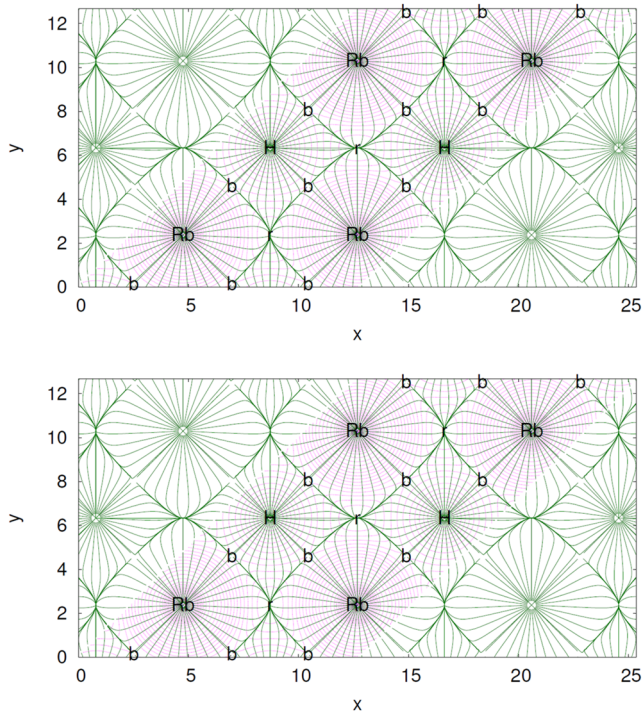

FIG. 5. ∇ρ trajectories of the gradients of the electron density (ρ). The density is divided into regions called basins. The green lines indicate the trajectories of each disjoint basin. The letter **nbcr** indicate the position of critical points which fulfill the zero-flux surfaces condition.

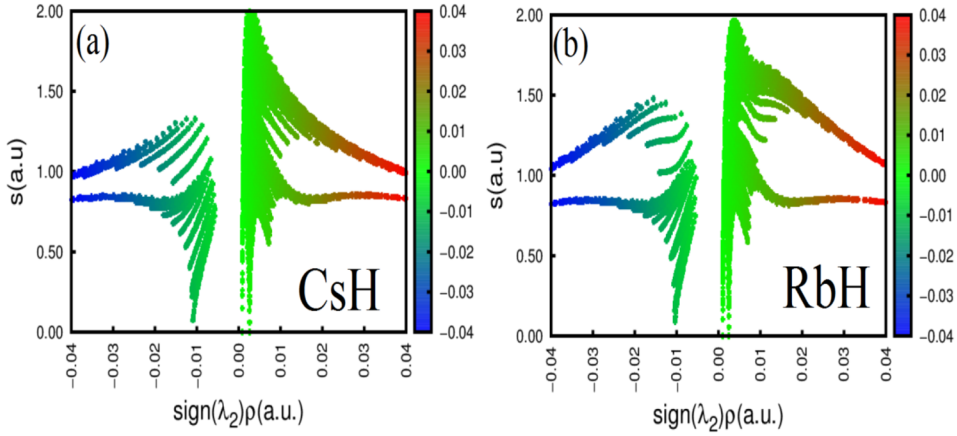

FIG. 6. 2D NCI plot for CsH and RbH compound in their NaCl phase.

the molecular structure.[34] In Figure 5, we plot the decomposition of the electron density obtained by the QTAIM approach of the studied compounds in their NaCl phase; in this plot basins are built by means of the crystal symmetry, which forces the existence of critical point at selected positions in the unit cell. By the use of semi-empirical relations proposed by Mori-Sánchez *et al.*,[35] ionicity index $\alpha = \frac{1}{N}\sum_{\Omega=1}^{N}\frac{Q(\Omega)}{OS(\Omega)}$ can be defined as an average for all the basins of the ratio between the local topological charge (Q(Ω)) (the net charge) and the nominal oxidation state(OS(Ω)). The predicted net charges of the CsH compound are respectively found equal to: -0.75 and 0.32 electrons for hydrogen and cesium ions. And for the RbH one, Q(Ω)= -0.73 and 0.34 electrons for the hydrogen and rubidium ions. The ionicity index is then equal to α(CsH) = 53.16% and α(RbH)= 53.98%. Here, the electrons of hydride ions are 75% transferred to the alkaline-earth metals. This behavior indicated that the bonds in our titled compounds are polar in their NaCl phase, with a mixing covalent-ionic character. At this stage, the fundamental question of the force practicing on the H–alkaline-earth metals bonds deserves a special attention. To answer such a question, we have made on the CsH and RbH compounds an additional analysis based on covalent interactions[36] to visualize the weak interactions based on the reduced electron density gradient RDG. The classification of the nature of the interaction is based on the sign of the second eigenvalue of the Hessian (λ_2) of the charge density. In fact, if $\lambda_2 < 0$ is negative; the attractions are judged to be attractive and colored in blue. However, if $\lambda_2 > 0$, the attractions are rather repulsive and colored in red color. In the case of the term of ($\lambda_2 \times \rho$) is close to zero, weak interactions are invoked and depicted in green color. The 2D and 3D plots of reduced density gradient (RDG) versus density multiplied by the sign of (λ_2) reveal clearly that the interactions are weak including dispersive forces. However, some hydrogen bonds are shown around the -0.01 in 2D map of RDG (see Figure 6) as well as in the 3D one of the CsH compounds (see Figure 7).

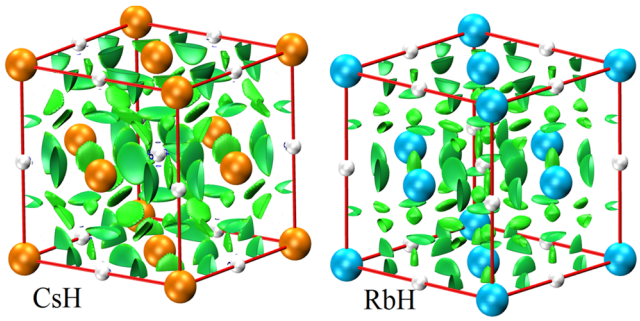

FIG. 7. 3D NCI plot for CsH and RbH compound in their NaCl phase.

D. Elastic properties

Elastic constants are crucial parameters, through their knowledge, one can predict and derive useful mechanical and thermodynamic properties such as brittleness, stiffness, shear's modulus (S), Young's modulus (Y), anisotropic ratio factor (A), Poisson's ratio (ν), Debye temperature (θ_D), transverse sound wave velocity (v_t), average sound wave velocity (v_m) and longitudinal sound wave velocity (v_l) for useful applications. To obtain elastic constants of RbH and CsH compounds in RS and CsCl structures, we used the method developed by Morteza Jamal and integrated in WIEN2k code.[13] The optimized lattice constants listed in Tables I and II have been used to estimate the elastic constants (C_{ij}) at zero temperature and at ambient pressure. This is done by forcing a small strain from -0.002 to 0.002 on the optimized unit cell and uses the energy approach to calculate the elastic constants. Because of the cubic crystal high symmetry, Rs and CsCl structures have only three independent elastic constants (C_{11},C_{12} and C_{44}). Calculated elastic constants and their related parameters as, bulk moduli (B), shear's modulus (S), Young's modulus (Y), anisotropic ratio factor (A), Poisson's ratio (ν), Debye temperature (θ_D), transverse velocity (v_t) and longitudinal velocity (v_m) of the RbH and CsH are displayed in Tables V and VI for the RS and CsCl structures; respectively along with the available previous theoretical results.[22,24,37] The values of the computed elastic moduli for RbH and CsH compounds in both RS and CsCl structure agree well with previous theoretical results. C_{12} for the RbH compound in the CsCl structure has a negative value; as Xinyou et al.[12] result of KH compound and Jaradat *et al.*[37] results of KH, RbH and CsH compounds; the results are to some extent consistent with Jaradat *et al.*,[37] Sudha *et al.*[24] and Xinyou *et al.*[12] results. The elastic constants in the RS and CsCl structures decrease as the alkali radii increase, which means CsH is less mechanically stronger. These compounds are mechanically stable in the RS and CsCl structures, they satisfy the Born mechanical stability criteria, the criteria for cubic structures are given by:[38]

$$C_{44} > 0,\ C_{11} > 0,\ C_{11} + 2C_{12} > 0;\ C_{11} > B > C_{12},\ \text{where B is the bulk modulus.}$$

Voigt (V) and Reuss (R) are two approximations usually used to estimate the mechanical and thermodynamic properties of materials.[39,40] These two approximations denoted the lower and upper limits of the mechanical and thermodynamic properties. Mechanical and thermodynamic properties can be predicted by employing Voigt-Reuss-Hill (VRH) approximation; VRH approximation indicates the arithmetic average of Voigt and Reuss.[41]

TABLE V. The calculated elastic constants (C_{ij} in GPa), Bulk modulus B (GPa) compressibility (β in GPa^{-1}), Shear modulus (S in GPa),Young's modulus (Y in GPa), Poisson's ratio (υ), B/S ratio, Anisotropic ratio (A), Debye temperature (θ_D in K), longitudinal elastic wave velocity (v_l in m/s), transverse elastic wave velocity (v_t in m/s) and average wave velocity (v_m in m/s) for RbH and CsH compounds in RS structure along with available theoretical data.

	RbH		CsH	
Elastic parameters	Present work	Other theoretical calculations	Present work	Other theoretical calculations
C_{11}	27.89	26.46[a], 28.2[b], 25.29[c]	24.38	25.6[a], 20.3[b], 20.7 [c]
C_{12}	3.65	7.93 [a], 7.11[b], 5.7[c]	3.84	6.76[a], 3.1[b], 3.17 [c]
C_{44}	10.58	10.97 [a], 12.5[b], 8.44[c]	10.13	9.74[a], 9.1[b], 8.0 [c]
B	11.73	13.97 [a], 11.81[c]	10.69	11.98[a], 9.02[c]
β	0.0852	0.0846[c]	0.0935	0.083[a], 0.1108[c]
S	11.19	10.2 [a], 9.10[c]	10.18	9.15[a], 8.31[c]
Y	25.48	25 [a], 21.73[c]	23.19	22[a], 19.0[c]
ν	0.138	0.23[a], 0.193[c]	0.138	0.22[a], 0.147[c]
B/S	1.048	1.37[a], 1.2978[c]	1.05	1.085[a], 1.085[c]
A	0.87	1.18[a], 0.834[c]	0.98	1.18[a], 0.912[c]
θ_D	222.0	215[a], 203.15[c]	175.8	167[a], 160.37[c]
v_l	3117	3225[a], 3039[c]	2630	2634[a], 2458[c]
v_t	2019	1959[a], 1872[c]	1704	1618[a], 1580[c]
v_m	2215	2165[a], 2065[c]	1869	1786[a], 1735[c]

[a]Reference 24,
[b]Reference 22,
[c]Reference 37.

TABLE VI. The calculated elastic constants (C_{ij} in GPa), Bulk modulus B (GPa) compressibility (β in GPa^{-1}), Shear modulus (S inGPa),Young's modulus (Y in GPa), Poisson's ratio (υ), B/S ratio, Anisotropic ratio (A), Debye temperature (θ_D in K), longitudinal elastic wave velocity (v_l in m/s), transverse elastic wave velocity (v_t in m/s) and average wave velocity (v_m in m/s) for RbH and CsH compounds in CsCl structure along with available theoretical data.

	RbH		CsH	
Elastic parameters	Present work	Other theoretical calculations	Present work	Other theoretical calculations
C_{11}	49.2	42[a], 52,73[b]	37.2	38[a], 38.21[b]
C_{12}	-3.1	1.4[a], -2.78[b]	2.8	3.2[a], -1.9[b]
C_{44}	5.8	12[a], 1.67[b]	4.0	6.5[a], 4.3[b]
B	14.3	14.85[a], 15.71[b]	14.3	13.97[a], 11.46[b]
β	0.0699	0.0636[b]	0.0699	0.0872[b]
S	10.9	15[a], 12.1[b]	8.4	11[a], 10.6[b]
Y	26.2	34[a], 28.9[b]	19.1	26[a], 24.3[b]
ν	0.195	0.03[a], 0.193[b]	0.233	0.07[a], 0.146[b]
B/S	1.31	0.99[a], 1.298[b]	1.7	1.27[a], 1.081[b]
A	0.22	0.060[a], 0.95[b]	0.23	0.07[a], 0.214[b]
θ_D	216.8	180[b]	148	158[b]
v_l	2965	2906[b]	2376	2427[b]
v_t	1825	1563[b]	1319	1479[b]
v_m	2013	1745[b]	1469	1634[b]

[a]Reference 24,
[b]Reference 37.

Shear modulus (S) describes the material's response to shear strain, in other words, this quantity represents material resistance against plastic deformation.[39,40]

The Hill shear modulus (S_H) is the arithmetic mean of the Voigt shear modulus (S_v) and the Reuss shear modulus (S_R). The Voigt shear modulus (S_v), the Reuss shear modulus (S_R)and the Hill shear modulus (S_H) are given by:

$$S_v = \frac{1}{5}(C_{11} - C_{12} + 3C_{44}) \tag{3}$$

$$S_R = \frac{5C_{44}(C_{11-C_{12}})}{4C_{44} + 3(C_{11-C_{12}})} \tag{4}$$

$$S_H = \frac{1}{2}(S_v + S_R) \tag{5}$$

The Young's modulus (Y) describes the material's response to linear strain and defined as the ratio of the stress to strain. It is an important parameter for technological and engineering application, it gives us information about the solid's stiffness, the larger the value of (Y) the stiffer the solid material is,[40] Young's modulus (Y) is given by:

$$Y = \frac{9S_H B}{(S_H + 3B)} \tag{6}$$

The bulk modulus (B) represents the resistance of solid to fracture, for cubic structures B is given by:

$$B = \frac{1}{3}(C_{11} + 2C_{12}) \tag{7}$$

From Tables V and VI, bulk moduli for RbH and CsH compounds are extremely small, which means RbH and CsH have a weak resistance to the fracture in the RS structure. RbH compound has more resistance to fracture (greater bulk modulus) than CsH compound. One can see that the CsCl structure is harder than RS structure, because CsCl structure possess a greater value of bulk modulus and lower value of compressibility (β=1/B). The values of the bulk moduli for RbH and CsH in the RS and CsCl computed from the Murnaghan's equation in Tables I and II are to some extent agree with the results obtained from elastic constants calculations. It can be seen from Tables V and VI that the values of the bulk moduli for RbH and CsH compounds in the RS and CsCl structures are greater than the

shear moduli. This means that shear moduli are the elastic parameters which limiting the mechanical stability of these compounds. Material's stiffness can be described by resistance to distortion; the greater the value of Young's modulus (Y) yields a harder material deformation, means the stiffer the material is. The calculated values of Young's moduli are represented in Tables V and VI, Young's moduli values indicate that the stiffness decreases as the alkali radii increase in the RS and CsCl structures. The RS structure is stiffer than the CsCl structure, this means that RS structure of RbH and CsH compounds is the more mechanically stronger than CsCl structure.

The elastic anisotropic factor (A) characterizes the anisotropy of the elastic wave velocity in a crystal and also describes the variation in crystal atomic arrangement in different directions.[42,43] A is unity for completely isotropic compound; A for cubic structures can be given by.

$$A = \frac{2C_{44}}{C_{11} - C_{12}} \tag{8}$$

From Table V, A for CsH in the RS structure is almost unity, which means CsH in the RS structure is almost completely isotropic, while RbH in the RS structure is not completely isotropic. Table VI represents the anisotropy factor for both RbH and CsH in the CsCl structure, A=0.22 and 0.23 for RbH and CsH, respectively. This means that these compounds are anisotropic in the CsCl structure.

Poisson's ratio (v) is an indicator which is used to judge the brittleness and ductility of the solid compounds, the critical value of v is 1/3, the compound has a ductile (brittle) nature when $v > 1/3$ ($v < 1/3$),.[44]

The Poisson's ratio (v) is given by:

$$v = \frac{3B - 2S_H}{2(3B + 2S_H)} \tag{9}$$

Poisson's ratio for RbH and CsH compounds is less than 1/3 in both RS and CsCl structures, means they have a brittle nature, present results agree with Ref. 24 that RbH and CsH compounds have a brittle nature in both RS and CsCl structures. Another simple relationship has been suggested by Pugh to judge whether the compound is brittle or ductile in nature.[44] Pugh relation based on the ratio of the bulk B to shear modulus S, if B/S>1.75 the compound behaves in ductile nature, otherwise the material has a brittle nature. B/S for the two compounds RbH and CsH in both RS and CsCl structures is lower than 1.75, this means that Pugh relation values for RbH and CsH in RS and CsCl are consistent with Poison's ratio that these compounds have a brittle nature.

Debye temperature (θ_D) of material defines as the highest temperature that can be accomplished as a result of single normal of vibration; it is given by:[41]

$$\theta_D = \frac{h}{k_B}\left[\frac{3n}{4\pi}\left(\frac{N_A\rho}{M}\right)\right]^{1/3} v_m \tag{10}$$

Where h is Plank's constant, k_B is Boltzmann's constant, N_A is Avogadro's number, ρ is the mass density per unit volume, M is the molecular weight, and v_m is average sound velocity. Average velocity (v_m), transverse velocity (v_l) and longitudinal velocity (v_t) of sound are given by:[45–47]

$$v_m = \left[\frac{1}{3}\left(\frac{2}{V_t^3} + \frac{1}{V_l^3}\right)\right]^{-1/3} \tag{11}$$

$$v_l = \sqrt{\frac{B + 4S/3}{\rho}} \tag{12}$$

$$v_t = \sqrt{S/\rho} \tag{13}$$

It is clear from Tables V and VI that the Debye temperature and the three sound wave velocities decrease as the alkali radius increases, also the value of these parameters in the RS structure are larger than their values in the CsCl structure. From the sound wave velocities relations, these velocities mainly depend on the shear modulus (S) and bulk modulus (B) values. As a result the sound velocity increases as the shear and bulk modulus increase.

E. Optical properties

Optical properties of XH compounds in the RS and CsCl structures are obtained from the frequency dependent complex dielectric function $\varepsilon(w)$ which is given by the Ehrenreich and Cohen's equation.[48]

$$\varepsilon(w) = \varepsilon_1(w) + i\varepsilon_2(w) \tag{14}$$

For small wave vector, the complex dielectric function measures the linear response of electron to an external electromagnetic field. There is an interaction between electric field of an incident photon and electron in crystal; interaction can be described by the time dependent perturbation of the ground state electronic states. The interaction of electric field of the incident photon with electron in crystal causes optical transitions between unoccupied and occupied states. The imaginary part ε_2 (ω) of the complex dielectric function can be obtained from the momentum dipole matrix elements between the occupied and the unoccupied electronic states wave functions. The real part $\varepsilon_1(w)$ of the complex dielectric function can be evaluated from the Kramer-Kronig relationship. The imaginary $\varepsilon_2(w)$ and real part $\varepsilon_1(w)$ of the complex dielectric function for cubic symmetry compound can be given by[49–51]

$$\varepsilon_1(w) = 1 + \frac{2}{\pi}\mathcal{P}\int_0^\infty \frac{w'\varepsilon_2(w)}{(w'^2 - w^2)}dw' \tag{15}$$

$$\varepsilon_2(w) = \frac{e^2\hbar}{\pi m^2 w^2}\sum_{v,c}\int_{BZ}|M_{cv}(k)|^2\delta(w_{cv} - w)d^3k \tag{16}$$

Where $\mathcal{P}$ represents the Cauchy principal value of the integral, $M_{cv}(k) = \langle u_{ck}|e.\nabla|u_{vk}\rangle$ represents the momentum dipole matrix of the incident electric field, e is the potential vector representing the electric field matrix for direct transition between u_{vk} and u_{ck} (valence and conduction band states) and $\hbar w_{cv}(k) = E_{ck} - E_{vk}$ is the transition energy.

Refractive index n(ω) is a frequency dependent function, it is an important physical parameter and closely related to the energy band structure of the material, it is obtained in terms of the real and imaginary parts of the dielectric function; $\varepsilon_1(w)$ and $\varepsilon_2(w)$; by the following relation:[49–51]

$$n(w) = \left(\frac{1}{2}\left[\sqrt{\varepsilon_1^2(w) + \varepsilon_2^2(w)} + \varepsilon_1(w)\right]\right)^{1/2} \tag{17}$$

Furthermore, others important optical parameters can be obtained immediately from ε_1(w) and $\varepsilon_2(w)$, reflectivity R(w), absorption coefficient α(w), extinction coefficient k(w) and energy loss spectrum L(w) and they can be given by:[49–51]

$$R(w) = \left|\frac{\sqrt{\varepsilon(w)} - 1}{\sqrt{\varepsilon(w)} + 1}\right|^2 = \left|\frac{\sqrt{\varepsilon_1 + i\varepsilon_2} - 1}{\sqrt{\varepsilon_1 + i\varepsilon_2} + 1}\right|^2 \tag{18}$$

$$\alpha(w) = \frac{\sqrt{2}w}{c}\left(\sqrt{\varepsilon_1^2(w) + \varepsilon_2^2(w)} - \varepsilon_1(w)\right)^{1/2} \tag{19}$$

$$k(w) = \left(\frac{1}{2}\left[\sqrt{\varepsilon_1^2(w) + \varepsilon_2^2(w)} - \varepsilon_1(w)\right]\right)^{1/2} \tag{20}$$

$$L(w) = \frac{\varepsilon_2(w)}{\varepsilon_1(w)^2 + \varepsilon_2(w)^2} \tag{21}$$

Figures 8 and 9 displaying the computed real part and imaginary part of the complex dielectric function for RbH and CsH compounds with the RS and CsCl structures, respectively. The static real dielectric constants $\varepsilon_1(0)$ of RbH with RS structure are about 2.37 (mBJ: 1.59) and 2.63 (mBJ: 1.83) with CsCl structure, while for CsH $\varepsilon_1(0)$ are about 2.37 (mBJ: 1.59) 2.63 (mBJ: 1.83), indicating that RbH and CsH with RS and CsCl are suitable as dielectric compounds. The real part of the dielectric constant ε1(w); for both RbH and CsH with RS and CsCl; are negative in a small regions, in these regions the photons are completely absorbed and this reflect a metallic nature in these regions. RS

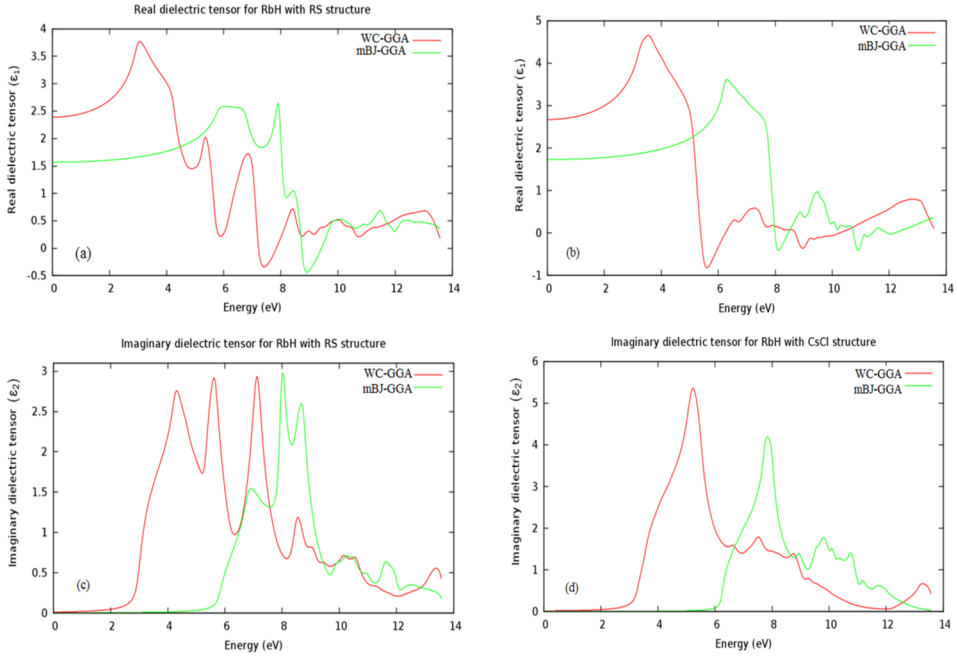

FIG. 8. Real dialectic constant ε_1(w) of RbH in a) RS b) CsCl structures, imaginary dialectic constant ε_2(w) of RbH in c) RS d) CsCl structures.

and CsCl structures have a different band structures, these differences lead to significantly various dielectric functions for both RbH and CsH, as shown in Figures 8 and 9. The $\varepsilon_2(w)$ for RbH with RS and CsCl onset at about 2.8eV and 3.2eV (mBJ: 5.75eV and 6.15eV) respectively, while for CsH $\varepsilon_2(w)$ with RS and CsCl structures onset at about 3.25eV and 3.78eV (mBJ: 5.65eV and 5.12eV)

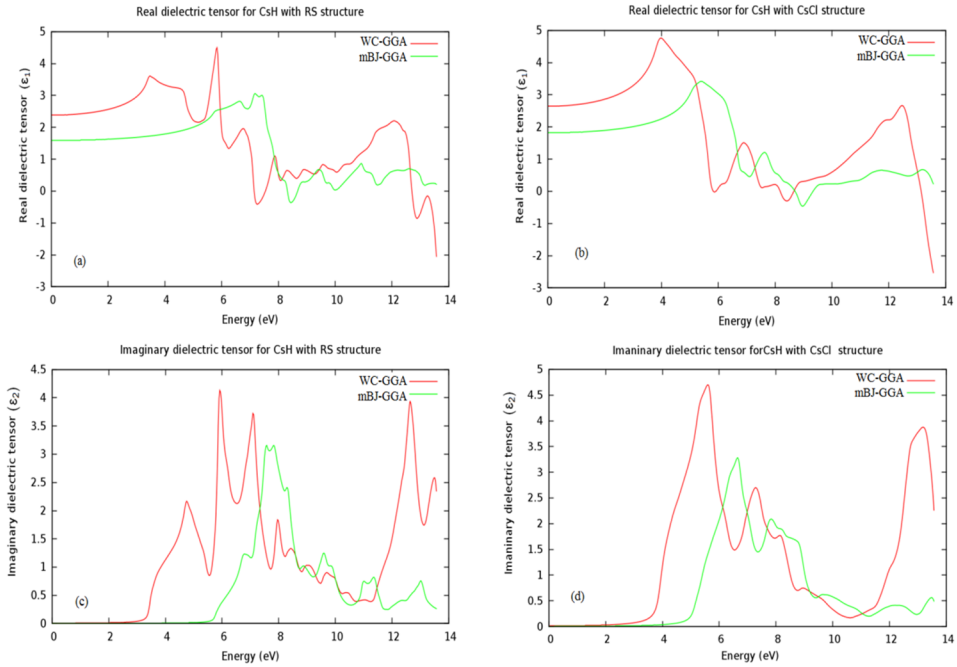

FIG. 9. Real dialectic constant ε_1(w) of CsH in a) RS b) CsCl structures, imaginary dialectic constant ε_2(w) of CsH in c) RS d) CsCl structures.

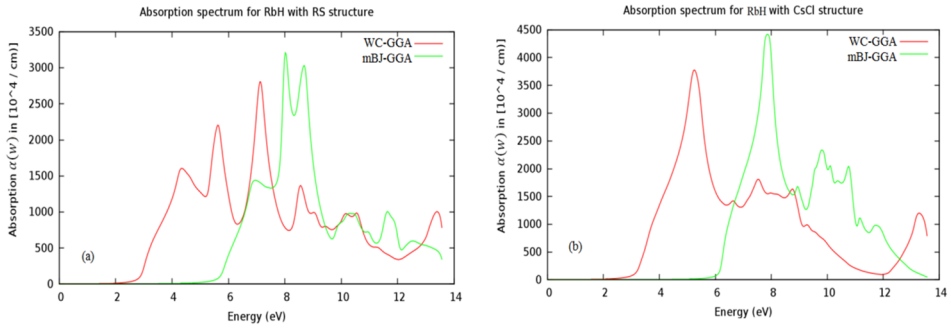

FIG. 10. Absorption coefficient $\alpha(w)$ of RbH in a) RS b) CsCl structures.

respectively, due to transitions at the L-point symmetry with RS structure and along the X-point symmetry with CsCl structure for the two compounds. The mBJ-GGA results for real and imaginary parts of the dielectric constant for both RbH and CsH are shifted toward to high energy direction, while the intensities are lower than those of WC-GGA. The first peaks in $\varepsilon_2(w)$ spectra for RbH with RS and CsCl structures are at energy approximately equals to 4.41eV and 5.18eV (mBJ: 6.8eV and 7.82eV) respectively, while for CsH are at about 4.8eV and 5.53eV (mBJ: 6.8eV and 6.6eV) respectively. It is noticeable that $\varepsilon_2(w)$ with RS structure has more peaks than CsCl structure for the two compounds; this is related to the variation in the energy band gap of the two structures. These peaks originate from the inter band transition, which is strongly related to the energy band gap. The peaks in imaginary dielectric function are due to electrons transitions from valence to conduction bands. RbH and CsH compounds have a wide direct energy band gaps, their maximum absorption are located in the middle ultraviolet (MUV4.13–6.20 eV) region and far ultraviolet (FUV12.4–6.20 eV) region, therefore they are could be suitable for the optoelectronic UV optoelectronic device applications including laser diodes (LDs) and light-emitting diodes (LEDs). The optical absorption coefficients $\alpha(w)$ of both RbH and CsH with RS and CsCl structures are displayed in Figures 10 and 11, respectively. Both of RbH and CsH with RS and CsCl structures have a wide absorption region, on the other hand RbH absorption is very huge compared with CsH absorption and this is related to the differences in the energy band gap. It is noticeable that the RbH is an excellent absorbent material. The maximum absorption regions are located in the middle ultraviolet (MUV) region and far ultraviolet (FUV) region. Optical absorptions of RbH with RS and CsCl start from about 2.9eV (mBJ: 5.3eV) and 3.2eV (mBJ: 6.1eV), respectively. For CsH absorption start from about 3.2eV (mBJ: 5.8eV) and 3.8eV (mBJ: 5.0eV), respectively. We can see that absorption begins when photon energy is close to the minimum direct energy band gap and no absorption is observed when the photon energy is less than the threshold absorption energy. Absorption curves of both RbH and CsH with RS and CsCl approaches using mBJ method move to high energy direction, with comparison with the WC- GGA approach. These two compounds are suitable as absorbing materials because they

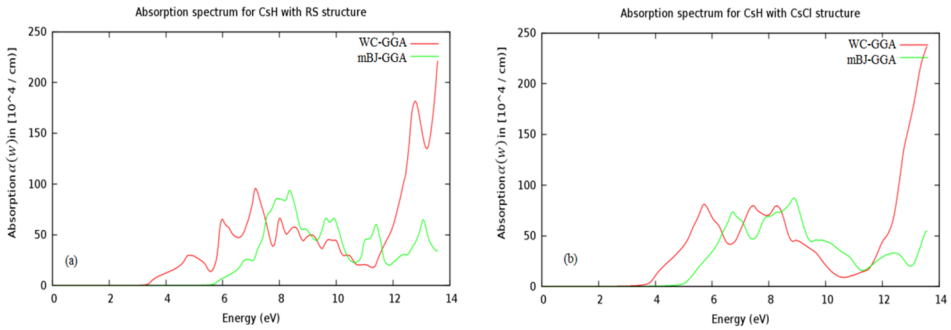

FIG. 11. Absorption coefficient $\alpha(w)$ of CsH in a) RS b) CsCl structures.

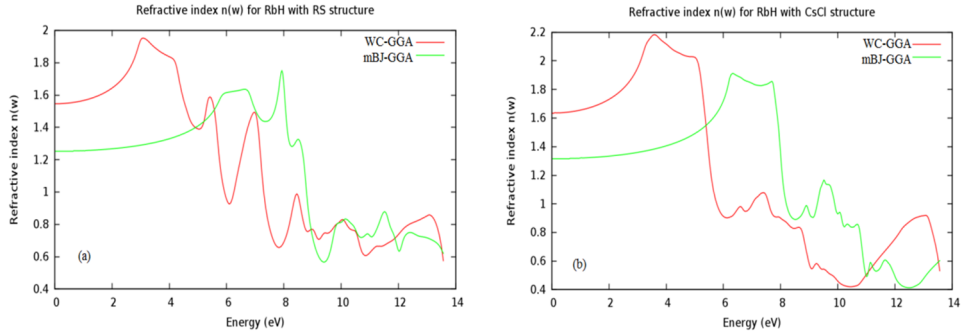

FIG. 12. Refractive index n(w) of RbH in a) RS b) CsCl structures.

have broad absorption regions, especially in the MUV and FUV regions. The calculated refractive index n(ω) for RbH and CsH with RS and CsCl structures are shown in Figures 12 and 13. The static refractive index n(0) for RbH with RS and CsCl structures are about 1.54 and 1.63 (mBJ: 1.25 and 1.31) respectively, and for CsH with RS and CsCl structures are about 1.55 and 1.62 (mBJ: 1.25 and 1.34) respectively. The refractive index n(ω) with mBJ move toward to high energy direction with lower intensities. Maximum refractive index n(ω) for RbH with RS and CsCl structures occurred at3.09eV and 3.60eV (mBJ:7.93eV and 6.26eV) respectively, while for CsH occurred at 5.84eV and 4.0eV (mBJ:7.47eV and 5.42eV) respectively. The calculated extinction coefficient k(ω) for RbH and CsH with RS and CsCl structures are shown in Figures 14 and 15, respectively. The absorption coefficient α(w), imaginary part of dielectric constant $\varepsilon_2(w)$ and the extinction coefficient k(w) vary in the same way, extinction coefficient k(w) stile zero until absorption begins. The reflectivity coefficient $R(\omega)$ for RbH and CsH with RS and CsCl structures are shown in Figures 16 and 17,

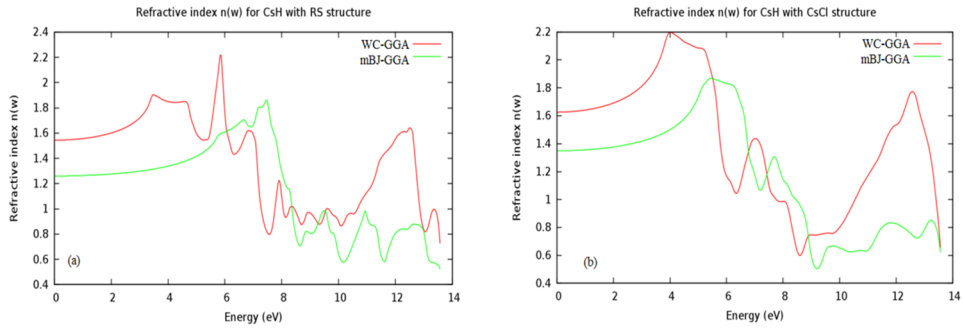

FIG. 13. Refractive index n(w) of CsH in a) RS b) CsCl structures.

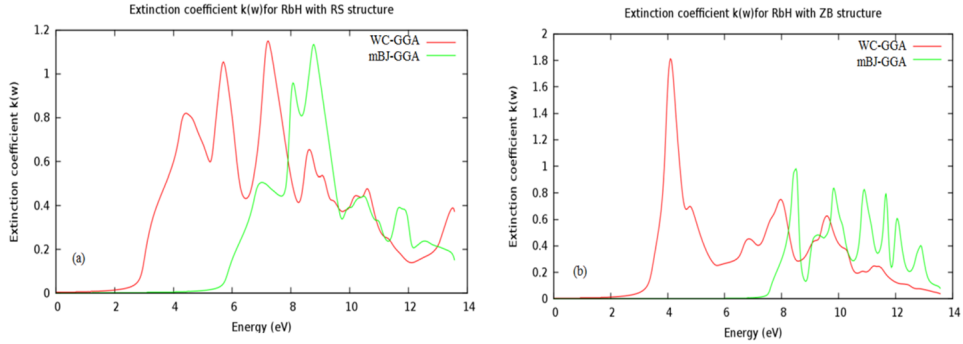

FIG. 14. Extinction coefficient $k(w)$ of RbH in a) RS b) CsCl structures.

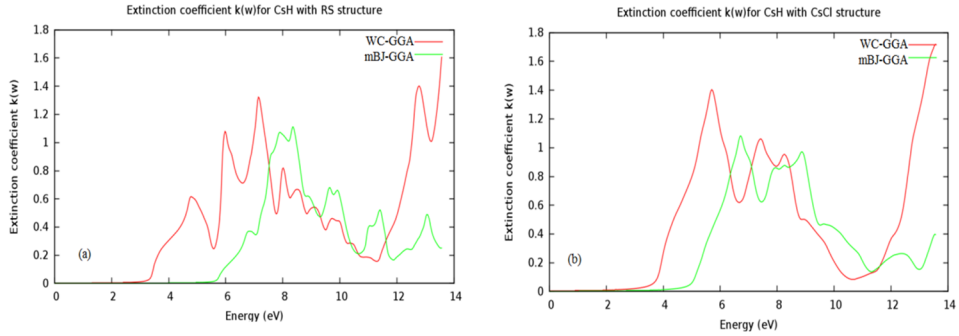

FIG. 15. Extinction coefficient $k(w)$ of CsH in a) RS b) CsCl structures.

respectively. The reflectivity parameter is an important coefficient, $R(\omega)$ displaying the percent of reflected energy at the solid surface. The static reflectivity $R(0)$ for both RbH and CsH with RS and CsCl is small, the zero-frequency reflectivity $R(0)$ for RbH with RS and CsCl are 4.5% and 5.6% (mBJ: 1.3% and 1.79%) respectively, while $R(0)$ for CsH with RS and CsCl structures are 4.5% and 5.6% (mBJ:1.3% and 1.8) respectively. It is clear that R(0) with WC-GGA greater than with mBJ approach. The energy loss function $L(\omega)$ for RbH and CsH with RS and CsCl structures are shown in Figures 18 and 19, respectively. The energy loss function L(ω) usually describing the energy loss of the fast electrons traversing in a material, L(ω) resonance peaks correspond to the plasma frequency.[52] Maximum peaks for the energy loss function for RbH with RS and CsCl structures occurred at 10.8 and 10.75eV (mBJ: 9.52 and 12.52eV) respectively, and for CsH occurred at 7.65 and 8.75eV (mBJ: 13.52 and 9.42eV). Comparing with the CsCl structure results, the L(ω) function with RS has more peaks, and this is related to the differences in energy band gap region. Maximum energy loss occurs

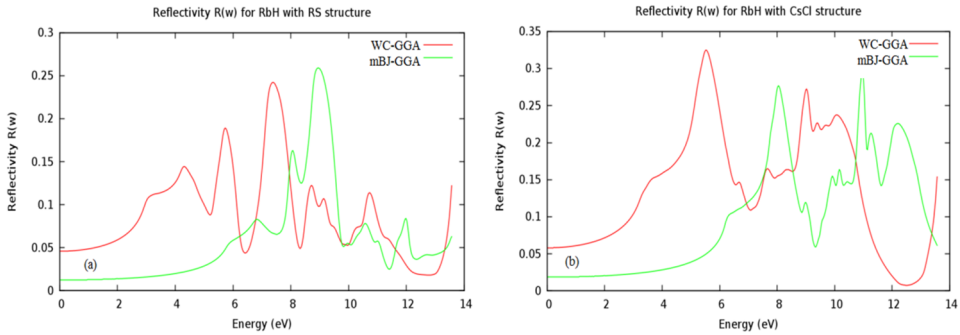

FIG. 16. Reflectivity $R(w)$ of RbH in a) RS and b) CsCl structures.

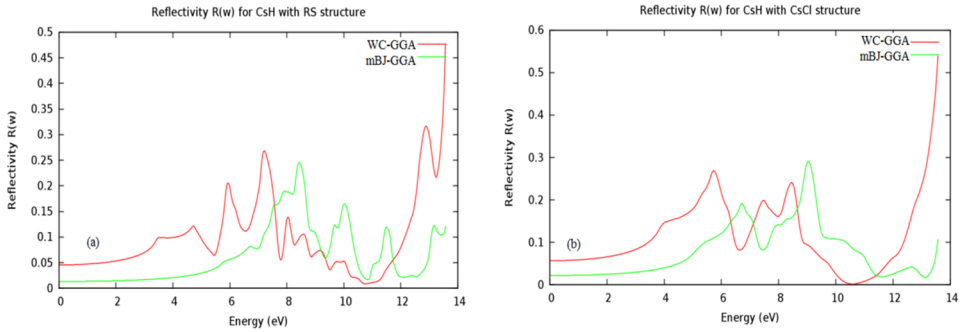

FIG. 17. Reflectivity $R(w)$ of CsH in a) RS and b) CsCl structures.

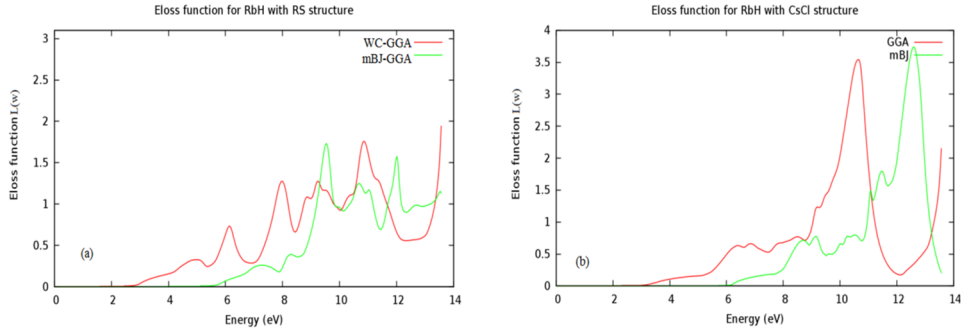

FIG. 18. Energy loss function $L(w)$ of RbH in a) RS and b) CsCl structures.

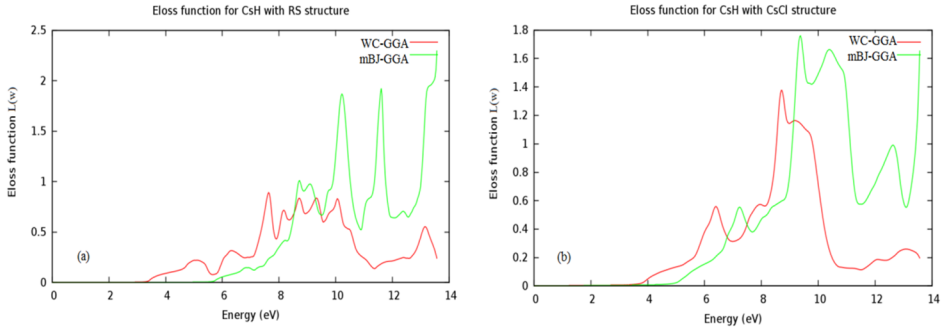

FIG. 19. Energy loss function $L(w)$ of CsH in a) RS and b) CsCl structures.

when the real part of the dielectric function $\varepsilon_1(\omega)$ is minimum, and when there is a rapid decrease in reflectivity $R(\omega)$. The two compounds have high energy absorption and high energy loss in the RS and CsCl structures, therefore, both RbH and CsH are suitable as wave absorbing compounds in the (MUV) and (FUV) regions, but unsuitable as transparent compounds.

IV. CONCLUSION

We have investigated the structural, electronic, elastic and optical properties of the RbH and CsH in RS and CsCl structures using WC-GGA method and found that these compounds can be treated as a dielectric compounds. RbH and CsH compounds are also found to be a wide direct energy band gap, therefore they could be suitable for the optoelectronic UV device applications. The RbH is found to be an excellent absorbent material. Both RbH and CsH compounds are suitable as absorbing materials because they have broad absorption regions, especially in the MUV and FUV regions. mBJ method shows that all optical curves for both RbH and CsH in RS and CsCl structures are moved to high energy direction compared to the WC-GGA method.

RbH and CsH compounds are mechanically stable; their elastic constants satisfy the Born–Huang criteria in the RS and CsCl structures. RbH compound has larger elastic constants than CsH compound in both RS and CsCl structures, which means RbH compound is more mechanically stronger than CsH compound, as the alkali radius increases it becomes mechanically less stronger. B/S value, Poisson's value as well as the bulk modulus small value for RbH and CsH compounds represent a brittle nature for RbH and CsH compounds. The Young's modulus value, indicates that the stiffness decreases as the alkali's radius increases. The RS structure is the stiffer than the CsCl structure, this means that RS structure of RbH and CsH compounds is the more mechanically stronger than CsCl structure which is consistence with elastic constants and the bulk moduli values. Debye temperature as well as the sound wave velocities decrease as the alkali radius increases, these parameters in RS structure has a larger value than CsCl structure for the two compounds.

ACKNOWLEDGMENTS

This work has been carried out in the Computational Physics Laboratory, Physics Department, An-Najah N. University.

[1] M. J. Latroche, "Structural and thermodynamic properties of metallic hydrides used for energy storage," Phys. Chem Solids. **65**, 517 (2004).
[2] Y. Oumellal, W. Zaïdi, J. P. Bonnet, F. Cuevas, M. Latroche, J. Zhang, J. L. Bobet, A. Rougier, and L. Aymard, Int. J. Hydrogen Energy **37**, 7831 (2012).
[3] S. I. Orimo, Y. Nakamori, J. R. Eliseo, A. Zuttel, and C. M. Jensen, Chem. Rev. **107**, 4111–4132 (2007).
[4] Y. Zhong and D. D. Macdonald, J. Nucl. Mater. **423**, 87 (2012).
[5] Z. W. Wang, Y. S. Yao, L. Zhu, H. Y. Liu, T. Litaka, H. Wang, and Y. M. Ma, J. Chem. Phys. **140**, 124707 (2014).
[6] S. Lebègue, C. M. Araújo, O. Eriksson, B. Arnaud, M. Alouani, and R. Ahuja, J. Phys.: Condens Matter **19**, 036223 (2007).
[7] K. Ghandehari, H. Luo, A. L. Ruoff, S. S. Trail, and F. J. DiSalvo, "New high pressure crystal structure and equation of state of cesium hydride," Phys. Rev. Lett. **74**, 2264 (1995).
[8] S. J. Duclos, Y. K. Vohra, A. L. Ruoff, S. Filipek, and B. Baronowski, "High-pressure studies of NaH to 54 GPa," Phys. Rev. B. **36**, 7664 (1987).
[9] H. D. Hochheimer, K. Strossner, W. Honle, B. Baranowski, and F. Filipek, "High pressure x-ray investigation of the alkali hydrides NaH, KH, RbH and CsH," Z. Phys. Chem. Neue Folge. **143**, 139 (1985).
[10] S. E. Gulebaglan, E. K. Dogan, M. N. Secuk, M. Aycibin, B. Erdinc, and H. Akkus, "First-principles study on electronic, optic, elastic, dynamic and thermodynamic properties of RbH compound," Int. J. Simul. Multisci. Des. Optim. **6**, A6 (2015) (http://creativecommons.org/licenses/by/4.0).
[11] M. J. van Setten, V. A. Popa, G. A. de Wijs, and G. Brocks, "Electronic structure and optical properties of lightweight metal hydrides," Phys. Rev. B **75**, 035204 (2007).
[12] A. Xinyoua *et al.*, "The mechanical, electronic and optical properties of KH under high pressure: A density functional theory study," 2017, Mater. Res. Express, at press.
[13] P. Blaha, K. Schwarz, G. Madsen, D. Kvasnika, and J. Luitz, *WIEN2k*, Technical Universitat Wien, Austria, 2001, ISBN 3-9501031-1-2.
[14] Z. Wu and R. E. Cohen, "More accurate generalized gradient approximation for solids," Phys. Rev. B **73**, 235116 (2006).
[15] A. Becke and M. Roussel, "Exchange holes in inhomogeneous systems: A coordinate-space model," Phys Rev A **39**, 3761 (1989).
[16] H. J. Monkhorst and J. D. Pack, "Special points for Brillonin-zone integrations," Phys. Rev. **13**, 5188 (1976).
[17] F. Tran, R. Laskowski, P. Blaha, and K. Schwarz, "Performance on molecules, surfaces, and solids of the Wu-Cohen GGA exchange-correlation energy functional," Phys. Rev. B **75**, 115131 (2007).
[18] E. Zintl and A. Harder, "Uber alkalihydride," Z. Phys. Chem. Abt. **14**, 265 (1931).
[19] W. Pearson, P. Villars, and L. D. Calvere, *Pearson's Handbook of Crystallographic Data for Intermetallic Phases* (ASM, Metals Park, Ohio, 1985).
[20] I. O. Bashkin, T. N. Dymova, and E. G. Ponyatovskii, "On the structural transition from NaCl to CsCl type in alkali hydrides," Phys. Status Solidi. **100**, 87 (1980).
[21] G. D. Barrera, D. Colognesi, P. C. H. Mitchell, and A. J. Ramirez-Cuesta, "LDA or GGA? A combined experimental inelastic neutron scattering and ab initio lattice dynamics study of alkali metal hydrides," Chem. Phys. **317**, 119 (2005).
[22] L. Engebretsen, "Electronic structure calculations of the elastic properties of alkali hydrides," Graduation Thesis, Royal Institute of Technology KTH, Stockholm, (1995).
[23] Z. Jingyun, Z. Lijun, C. Tian, L. Yan, H. Zhi, M. Yanming, and Z. Guangtian, "Phonon and elastic instabilities in rocksalt alkali hydrides under pressure: A first-principles study," Phys. Rev. B **75**, 104115 (2007).
[24] P. G. Sudha, A. T. Asvini, R. Rajeswara, and K. Iyakutti, "Structural, electronic and elastic properties of alkali hydrides (MH: M = Li, Na, K, Rb, Cs): Ab initio study," Comput. Mater. Sci. **84**, 206 (2014).
[25] S. Srinivasa Murthy and E. Anil Kumar, "Advanced materials for solid state hydrogen storage: 'Thermal engineering issues,'" Applied Thermal Engineering **72**, 176–189 (2014).
[26] J. P. Perdew and A. Zunger, "Self-interaction correction to density-functional approximations for many-electron systems," Phys. Rev. **23**, 5048 (1981).
[27] V. Luana and L. Pueyo, "Simulation of ionic crystals: The ab initio perturbed-ion method and application to alkali hydrides and halides," Phys. Rev. B **41**, 3800 (1990).
[28] N. Novakovic, I. Radisavljevic, D. Colognesi, S. Ostojic, and N. Ivanovic, "First principle calculations of alkali hydride electronic structures," J. Phys. Cond. Mat. **19**, 406211 (2007).
[29] R. C. Bowman, "Cohesive energies of the alkali hydrides and deuterides," J. Phys. Chem. **75**, 1251 (1971).
[30] P. Vajeeston, *Theoretical Modeling of Hydrides*, PhD thesis, University of Oslo, 2004.
[31] K. Ghandehari, H. Luo, A. L. Ruoff, S. S. Trail, and F. J. DiSalvo, "Crystal structure and band gap of rubidium hydride to 120 GPa," Mod. Phys. Lett. **9**, 1133 (1995).
[32] K. Ghandehari, H. Luo, A. L. Ruoff, S. S. Trail, and F. J. DiSalvo, "Band gap and index of refraction of CsH to 251 GPa," Solid State Commun. **95**, 385 (1995).
[33] M. Peruzzini and R. Poli, *Recent Advances in Hydride Chemistry* (Elsevier, St. Louis, 2001).
[34] R. F. W. Bader, *Atoms in Molecules: A Quantum Theory* (Oxford University Press, Oxford, 1990).
[35] P. Mori-Sánchez, A. Martín Pendás, and V. Luaña, J. Am. Chem. Soc. **124**, 14721 (2002).
[36] E. R. Johnson, S. Keinan, P. Mori-Sánchez, J. Contreras-García, A. J. Cohen, and W. Yang, "Revealing noncovalent interactions," J. Am. Chem. Soc **132**, 6498 (2010).
[37] R. Jaradat, M. S. Abu-Jafar, I. Abdelraziq, D. Dahliah, and R. Khenata, "Elastic and thermodynamic properties of alkali hydrides XH (X= K, Rb and Cs)."

[38] M. Born and K. Huang (Oxford: Clarendon) (1956).
[39] W. Voigt Wied, Ann Phys. **38**, 573 (1889).
[40] A. Reuss, Math. Phys. **9**, 49 (1929).
[41] R. Hill, Proc. Phys. Soc. London, Section A **65**, 349 (1952).
[42] C. Zener, *Elasticity and Anelasticity of Metals* (University of Chicago Press, Chicago, 1948).
[43] H. Xao, Y. Xu, Z. Wu, D. Zhou, X. Liu, and J. Meng, J Alloy Compd. **453**, 413 (2008).
[44] S. Pugh, The London, Edinburgh, and Dublin Philosophical Magazine J Sci **45**, 823 (1954).
[45] P. Wachter, M. Filzmoser, and J. Rebizant, Physica B **293**, 199 (2001).
[46] O. Anderson, E. Schreiber, and N. Soga, *Elastic constants, and their measurements* (McGraw-Hill, New York, 1973).
[47] C. Jasiukiewicz and V. Karpus, Solid State Commun. **128**, 167 (2003).
[48] H. Ehrenreich and M. H. Cohen, "Self-consistent field approach to the many-electron problem," Phys. Rev. **115**, 786 (1959).
[49] M. Fox, *Optical Properties of Solids* (Oxford University Press, New York, 2001).
[50] F. Wooten, *Optical Properties of Solids* (Academic Press, New York, 1972).
[51] H. Wang, Y. F. Wang, X. W. Cao, L. Zhang, M. Feng, and G. X. Lan, Phys. Status Solidi B **246**, 437 (2009).
[52] O. L. Anderson, "A simplified method for calculating the debye temperature from elastic constants," J. Phys. Chem. Solid **24**, 909 (1963).